Investigation of possible correlation between α-particle preformation probability and energy levels for α emitters with $74 \leqslant Z \leqslant 83$

M. Ismail[1,*] and A. Adel[1,2,†]

[1]*Physics Department, Faculty of Science, Cairo University, Giza, Egypt*

[2]*Physics Department, College of Science, Majmaah University, Al-Zulfi, Kingdom of Saudi Arabia*

(Received 23 October 2014; revised manuscript received 6 December 2014; published 31 December 2014)

The preformation probability of an α cluster inside radioactive parent nuclei is investigated. The calculations are employed in the framework of the density-dependent cluster model for both even-even and odd-A isotopes with $74 \leqslant Z \leqslant 83$. A realistic density-dependent nucleon-nucleon (NN) interaction with a finite-range exchange part is used to calculate the microscopic α-nucleus potential in the well-established double-folding model. The main effect of antisymmetrization under exchange of nucleons between the α and daughter nuclei has been included in the folding model through the finite-range exchange part of the NN interaction. The calculated potential is then implemented to find both the assault frequency and the penetration probability of the α particle by means of the Wentzel-Kramers-Brillouin approximation in combination with the Bohr-Sommerfeld quantization condition. We investigated the correlation between the α-particle preformation probability, S_α, and the energy levels of the parent nucleus for α emitters with atomic number $74 \leqslant Z \leqslant 83$. Based on the similarity in the behavior of S_α with the neutron number for two nuclei, we try to predict or confirm the unknown or doubted nuclear spins and parities in this mass region.

DOI: 10.1103/PhysRevC.90.064624 PACS number(s): 23.60.+e, 21.10.Tg, 21.10.Jx, 21.10.Hw

I. INTRODUCTION

Among various decay modes, α decay is the prominent one for heavy and superheavy nuclei and acts as an effective probe for the nuclear structure [1–7]. It can provide reliable information on ground-state lifetime, nuclear charge radius, nuclear incompressibility, nuclear spin, and parity [1,8,9]. It can also be used to identify new isotopes or new elements via the observation of an α decay chain from an unknown parent nucleus to a known daughter nucleus [10–12].

The α decay process is treated conventionally in the framework of the Gamow model [13] assuming a sub-barrier penetration of α particles through the Coulomb barrier, caused by interactions between α particles and the daughter nucleus. Following the pioneering quantum explanation of α decay as a tunneling effect, many effective theoretical approaches have been established to pursue a reasonable description of α decay. The generalized liquid-drop model (GLDM) [14], the density-dependent cluster model (DDCM) [15], the coupled channel approach [16,17], and the Coulomb and proximity potential model [18–20] are widely used in the decay study.

An interesting aspect in α decay is how to estimate the preformation probability, S_α, which gives the probability that the α particle exists as a recognizable entity inside the nucleus before its emission [21]. It is expected to reflect the influences of the different nuclear structure properties of the parent nucleus and its decay components, such as their isospin asymmetry [22] and shell and pairing effects [23]. The preformation probability, S_α, has been calculated as the ratio of the calculated half-life to the experimentally observed value.

In a previous work [5,24,25], we studied the correlation between α particle preformation probability, S_α, and the energy levels of parent nuclei with atomic number $Z \geqslant 84$. We found that S_α has a regular behavior with the neutron number variation if the neutron pair in α particles, emitted from adjacent isotopes, comes from the same energy level or from a group of levels, assuming that the order of levels in this group is not changed. Irregular behavior in S_α with neutron number occurs if the levels of the adjacent isotopes change or holes are created in lower levels. We also found that [25], for some cases, the measure of the neutron-proton (n-p) interaction of the two emission levels is too small for a regular variation of S_α, while it increases for a rapid change in the value of S_α. Irregular variation (sudden increase or decrease) in S_α becomes strong when both the neutron and proton levels are changed during the α emission process. Above the neutron magic number, $N = 126$, S_α increased with increasing number of neutrons in the level, but below $N = 126$ S_α decreases with decreasing number of neutrons (increasing number of holes) in the level $2f_{5/2}$ [25]. The level $3p_{3/2}$, below the level $2f_{5/2}$, is filled more than one time, leaving holes in the lower levels [24]. Also when the level $1i_{13/2}$ contributes to the α emission process, S_α jumps in its value for the odd neutron number isotopes.

The aim of the present paper is to try to find a correlation between S_α and the energy levels of the parent nucleus for α emitters with atomic number $74 \leqslant Z \leqslant 83$. Based on the above mentioned correlation, we try to confirm or predict the value of the (nuclear) spin of an element from the neutron number variation of S_α for the isotopes of this element. It should be noted that most of the nuclei in this atomic number region have spins imprecisely determined. The tabulated spin of an element has more than one value, in some cases, and some of the spins in this region are taken from extrapolation with neighboring nuclides and no experimental values are available.

*myi2000@hotmail.com

†Corresponding author: ahmedshosha200@yahoo.com, aa.ahmed@mu.edu.sa

The outline of the paper is as follows. In Sec. II a description of the microscopic nuclear and Coulomb potentials between the α and daughter nuclei is given. The methods for determining the decay width, the penetration probability, the assault frequency, and the preformation probability are also presented. In Sec. III, the calculated results are discussed. Finally, Sec. IV gives a brief conclusion.

II. THEORETICAL FRAMEWORK

In the performed cluster models, the α particle is considered to be formed with a definite probability as an individual cluster inside the parent nucleus at the preliminary stage. Once formed, it will try to emit, leaving the daughter nucleus behind. The α decay partial half-lifetime, $T_{1/2}$, of the parent nucleus is given in terms of the α decay width, Γ, as

$$T_{1/2} = \frac{\hbar \ln 2}{\Gamma}. \tag{1}$$

The absolute α decay width is mainly determined by the barrier penetration probability (P_α), the assault frequency (ν), and the preformation probability (S_α), $\Gamma = \hbar\, S_\alpha\, \nu\, P_\alpha$. The barrier penetration probability, P_α, could be calculated as the barrier transmission coefficient of the well-known Wentzel-Kramers-Brillouin (WKB) approximation, which works well at energies well below the barrier:

$$P_\alpha = \exp\left(-2 \int_{R_2}^{R_3} \mathrm{d}r \sqrt{\frac{2\,\mu}{\hbar^2} |V_T(r) - Q_\alpha|} \right). \tag{2}$$

Here μ is the reduced mass and Q_α is the Q value of the α decay. R_i ($i = 1,2,3$) are the three turning points for the α-daughter potential barrier where $V_T(r)|_{r=R_i} = Q_\alpha$.

The assault frequency of the α particle, ν, can be expressed as the inverse of the time required to traverse the distance back and forth between the first two turning points, R_1 and R_2, as [26]

$$\nu = T^{-1} = \frac{\hbar}{2\,\mu} \left[\int_{R_1}^{R_2} \frac{\mathrm{d}r}{\sqrt{\frac{2\mu}{\hbar^2} |V_T(r) - Q_\alpha|}} \right]^{-1}. \tag{3}$$

The total interaction potential of the α-core system comprises the nuclear and the Coulomb potentials plus the centrifugal part, and is given by [8,15]

$$V_{\mathrm{T}}(R) = \lambda\, V_N(R) + V_C(R) + \frac{\hbar^2}{2\,\mu} \frac{\left(\ell + \frac{1}{2}\right)^2}{R^2}, \tag{4}$$

where the renormalization factor λ is the depth of the nuclear potential, and R is the separation distance between the mass center of the α particle and the mass center of the core. The latter term in Eq. (4) represents the Langer modified centrifugal potential, μ is the reduced mass of the cluster-core system, and ℓ is the angular momentum carried by the α particle. The value of angular momentum ℓ, which is used for the calculation of the centrifugal term, is arranged in column five of Table I. These are the minimum values of possible angular momenta; the α particle can transfer any value of the angular momentum according to the following spin-parity selection rule:

$$|J_i - J_f| \leqslant \ell \leqslant |J_i + J_f| \quad \text{and} \quad \frac{\pi_f}{\pi_i} = (-1)^\ell, \tag{5}$$

where J_i, π_i and J_f, π_f are the spin and parity of parent and daughter nuclei, respectively.

The nuclear part of the potential, $V_N(R)$, consists of two terms: the direct, $V_D(R)$, and the exchange, $V_{\mathrm{Ex}}(R)$, terms. The direct part of the nuclear interaction potential between two colliding nuclei and the equation describing the Coulomb interaction have similar forms involving only diagonal elements of the density matrix [27,28]:

$$V_D(R) = \int d\vec{r}_1 \int d\vec{r}_2 \rho_\alpha(\vec{r}_1)\, \upsilon_D(\rho, E, s)\, \rho_d(\vec{r}_2), \tag{6}$$

where $s = r_2 - r_1 + R$ is the relative distance between a constituent nucleon in the α particle and one in the daughter nucleus. E is the incident laboratory energy per nucleon. $\rho_\alpha(\vec{r}_1)$ and $\rho_d(\vec{r}_2)$ are, respectively, the density distributions of the α particle and the residual daughter nucleus as described in Ref. [15].

The exchange potential accounts for the knock-on exchange of nucleons between the interacting nuclei. The exchange term is, in general, nonlocal. However, an accurate local approximation can be obtained by treating the relative motion locally as a plane wave [29,30]:

$$V_{\mathrm{Ex}}(E,R) = \int d\vec{r}_1 \int d\vec{r}_2 \rho_\alpha(\vec{r}_1, \vec{r}_1 + \vec{s})\, \rho_d(\vec{r}_2, \vec{r}_2 - \vec{s}) \times \upsilon_{\mathrm{Ex}}(\rho, E, s) \exp\left[\frac{i\vec{k}(R) \cdot \vec{s}}{M} \right]. \tag{7}$$

Here $k(R)$ is the relative-motion momentum given by

$$k^2(R) = \frac{2\,\mu}{\hbar^2} \left[E_{\mathrm{c.m.}} - V_N(E,R) - V_C(R) \right], \tag{8}$$

where μ is the reduced mass for the reacting nuclei, and $E_{\mathrm{c.m.}}$ is the center-of-mass (c.m.) energy. $V_N(E,R) = V_D(E,R) + V_{Ex}(E,R)$ and $V_C(R)$ are the total nuclear and Coulomb potentials, respectively. The folded potential is energy dependent and nonlocal through its exchange term and contains a self-consistency problem because the relative-motion momentum, $k(R)$, depends upon the total nuclear potential, $V_N(E,R) = V_D(E,R) + V_{Ex}(E,R)$, itself. This problem is solved by the iteration method. The exact treatment of the nonlocal exchange term is complicated numerically, but one may obtain an equivalent *local* potential by using a realistic localized expression for the nonlocal density matrix (DM) [29,30]:

$$\rho(\vec{r}, \vec{r} + \vec{s}) \simeq \rho\left(\vec{r} + \frac{\vec{s}}{2}\right)\, \hat{j}_1\left(k_{\mathrm{eff}}\left(\vec{r} + \frac{\vec{s}}{2}\right) s\right), \tag{9}$$

with

$$\hat{j}_1(x) = 3\, j_1(x)/x = 3(\sin x - x \cos x)/x^3. \tag{10}$$

The α particle is a unique case where a simple Gaussian can reproduce very well its ground state density [27]. Assuming four nucleons to occupy the lowest $s\frac{1}{2}$ harmonic oscillator shell in ^{4}He, one obtains exactly the nondiagonal ground state DM

TABLE I. The preformation probability, S_α, and the α-decay half-lives, $T_{1/2}^{\rm calc}$, calculated without S_α for W, Os, Pt, Hg, Pb, and Bi isotopes using the CDM3Y1-Paris NN interaction. Experimental Q values, α decay half-lives, spins, and parities are taken from Ref. [34]. Uncertain spin and/or parity assignments are in parentheses. The sign * means the spin and/or parity assignments as well as the angular momentum of transition are modified according to the behavior of S_α and their modified values are in brackets beside the used values in our calculations. The sign † means the tabulated spin is confirmed by the behavior of S_α.

Reaction	$Q_\alpha^{\rm expt}$ (MeV)	J_i^π	J_f^π	$\ell_{\rm min}$	$T_{1/2}^{\rm expt}$ (s)	$T_{1/2}^{\rm calc}$ (s)	S_α
$^{158}W \rightarrow {}^{154}Hf + \alpha$	6.6130	0^+	0^+	0	1.25×10^{-3}	1.14×10^{-4}	0.091
$^{159}W \rightarrow {}^{155}Hf + \alpha$	6.4500	$(7/2^-)^\dagger$	$(7/2^-)$	0	7.31×10^{-3}	4.08×10^{-4}	0.056
$^{160}W \rightarrow {}^{156}Hf + \alpha$	6.0650	0^+	0^+	0	1.05×10^{-1}	1.08×10^{-2}	0.103
$^{161}W \rightarrow {}^{157}Hf + \alpha$	5.9230	$(7/2^-)^\dagger$	$(7/2^-)$	0	4.76×10^{-1}	3.84×10^{-2}	0.081
$^{162}W \rightarrow {}^{158}Hf + \alpha$	5.6770	0^+	0^+	0	2.48×10^{0}	4.01×10^{-1}	0.162
$^{163}W \rightarrow {}^{159}Hf + \alpha$	5.5200	$7/2^-$	$7/2^-$	0	1.91×10^{1}	1.93×10^{0}	0.101
$^{164}W \rightarrow {}^{160}Hf + \alpha$	5.2785	0^+	0^+	0	1.66×10^{2}	2.55×10^{1}	0.154
$^{165}W \rightarrow {}^{161}Hf + \alpha$	5.0300	$(5/2^-)[3/2^{-*}]$	$(3/2^-)$	2[0*]	2.55×10^{3}	8.74×10^{2}	0.343
$^{166}W \rightarrow {}^{162}Hf + \alpha$	4.8560	0^+	0^+	0	4.80×10^{4}	3.72×10^{3}	0.078
$^{167}W \rightarrow {}^{163}Hf + \alpha$	4.7400	$3/2^-$	$3/2^-$	0	4.98×10^{4}	1.63×10^{4}	0.327
$^{161}Os \rightarrow {}^{157}W + \alpha$	7.0660	$(7/2^-)^\dagger$	$(7/2^-)$	0	6.40×10^{-4}	2.50×10^{-5}	0.039
$^{162}Os \rightarrow {}^{158}W + \alpha$	6.7670	0^+	0^+	0	2.12×10^{-3}	2.32×10^{-4}	0.109
$^{163}Os \rightarrow {}^{159}W + \alpha$	6.6800	$(7/2^-)^\dagger$	$(7/2^-)$	0	5.50×10^{-3}	4.44×10^{-4}	0.081
$^{164}Os \rightarrow {}^{160}W + \alpha$	6.4790	0^+	0^+	0	2.14×10^{-2}	2.22×10^{-3}	0.104
$^{165}Os \rightarrow {}^{161}W + \alpha$	6.3400	$(7/2^-)^\dagger$	$(7/2^-)$	0	8.88×10^{-2}	7.00×10^{-3}	0.079
$^{166}Os \rightarrow {}^{162}W + \alpha$	6.1390	0^+	0^+	0	2.76×10^{-1}	4.04×10^{-2}	0.146
$^{167}Os \rightarrow {}^{163}W + \alpha$	5.9800	$(7/2^-)^\dagger$	$7/2^-$	0	1.42×10^{0}	1.71×10^{-1}	0.120
$^{168}Os \rightarrow {}^{164}W + \alpha$	5.8160	0^+	0^+	0	4.88×10^{0}	8.13×10^{-1}	0.166
$^{169}Os \rightarrow {}^{165}W + \alpha$	5.7130	$(5/2^-)[7/2^{-*}]$	$(5/2^-)$	0[2*]	3.30×10^{1}	2.21×10^{0}	0.067
$^{170}Os \rightarrow {}^{166}W + \alpha$	5.5370	0^+	0^+	0	7.76×10^{1}	1.35×10^{1}	0.173
$^{171}Os \rightarrow {}^{167}W + \alpha$	5.3710	$(5/2^-)^\dagger$	$(5/2^-)$	0	4.94×10^{2}	8.03×10^{1}	0.163
$^{172}Os \rightarrow {}^{168}W + \alpha$	5.2240	0^+	0^+	0	9.60×10^{3}	4.19×10^{2}	0.044
$^{173}Os \rightarrow {}^{169}W + \alpha$	5.0550	$(5/2^-)$	$(5/2^-)$	0	5.60×10^{3}	3.10×10^{3}	0.553
$^{174}Os \rightarrow {}^{170}W + \alpha$	4.8700	0^+	0^+	0	2.2×10^{5}	3.14×10^{4}	0.143
$^{186}Os \rightarrow {}^{182}W + \alpha$	2.8204	0^+	0^+	0	6.31×10^{22}	7.56×10^{21}	0.120
$^{166}Pt \rightarrow {}^{162}Os + \alpha$	7.2860	0^+	0^+	0	3.00×10^{-4}	3.04×10^{-5}	0.101
$^{167}Pt \rightarrow {}^{163}Os + \alpha$	7.1600	$(7/2^-)$	$(7/2^-)$	0	9.00×10^{-4}	7.33×10^{-5}	0.081
$^{168}Pt \rightarrow {}^{164}Os + \alpha$	6.9900	0^+	0^+	0	2.03×10^{-3}	2.53×10^{-4}	0.125
$^{169}Pt \rightarrow {}^{165}Os + \alpha$	6.8580	$(7/2^-)^\dagger$	$(7/2^-)$	0	7.00×10^{-3}	6.81×10^{-4}	0.097
$^{170}Pt \rightarrow {}^{166}Os + \alpha$	6.7070	0^+	0^+	0	1.41×10^{-2}	2.21×10^{-3}	0.157
$^{171}Pt \rightarrow {}^{167}Os + \alpha$	6.6070	$(7/2^-)^\dagger$	$(7/2^-)$	0	5.06×10^{-2}	4.87×10^{-3}	0.096
$^{172}Pt \rightarrow {}^{168}Os + \alpha$	6.4640	0^+	0^+	0	1.04×10^{-1}	1.59×10^{-2}	0.153
$^{173}Pt \rightarrow {}^{169}Os + \alpha$	6.3500	$(5/2^-)[7/2^{-*}]$	$(5/2^-)$	0[2*]	4.60×10^{-1}	4.17×10^{-2}	0.090
$^{174}Pt \rightarrow {}^{170}Os + \alpha$	6.1830	0^+	0^+	0	1.20×10^{0}	1.83×10^{-1}	0.153
$^{175}Pt \rightarrow {}^{171}Os + \alpha$	6.1780	$7/2^-$	$(5/2^-)$	2	3.95×10^{0}	3.53×10^{-1}	0.089
$^{176}Pt \rightarrow {}^{172}Os + \alpha$	5.8850	0^+	0^+	0	1.58×10^{1}	3.03×10^{0}	0.191
$^{177}Pt \rightarrow {}^{173}Os + \alpha$	5.6430	$5/2^-$	$(5/2^-)$	0	2.12×10^{2}	3.59×10^{1}	0.169
$^{178}Pt \rightarrow {}^{174}Os + \alpha$	5.5729	0^+	0^+	0	5.18×10^{2}	7.39×10^{1}	0.143
$^{179}Pt \rightarrow {}^{175}Os + \alpha$	5.4120	$1/2^-$	$(5/2^-)$	2	8.83×10^{3}	8.26×10^{2}	0.094
$^{180}Pt \rightarrow {}^{176}Os + \alpha$	5.2400	0^+	0^+	0	2.00×10^{4}	3.12×10^{3}	0.156
$^{181}Pt \rightarrow {}^{177}Os + \alpha$	5.1500	$1/2^-$	$1/2^-$	0	7.32×10^{4}	9.00×10^{3}	0.123
$^{182}Pt \rightarrow {}^{178}Os + \alpha$	4.9510	0^+	0^+	0	4.58×10^{5}	1.09×10^{5}	0.239
$^{171}Hg \rightarrow {}^{167}Pt + \alpha$	7.6680	$(3/2^-)$	$(7/2^-)$	2	5.90×10^{-5}	2.24×10^{-5}	0.379
$^{172}Hg \rightarrow {}^{168}Pt + \alpha$	7.5240	0^+	0^+	0	2.31×10^{-4}	3.14×10^{-5}	0.136
$^{173}Hg \rightarrow {}^{169}Pt + \alpha$	7.3780	$(7/2^-)[5/2^{-*}]$	$(7/2^-)$	0[2*]	6.00×10^{-4}	8.55×10^{-5}	0.142
$^{174}Hg \rightarrow {}^{170}Pt + \alpha$	7.2330	0^+	0^+	0	2.11×10^{-3}	2.39×10^{-4}	0.114
$^{175}Hg \rightarrow {}^{171}Pt + \alpha$	7.0720	$(7/2^-)^\dagger$	$(7/2^-)$	0	1.07×10^{-2}	7.83×10^{-4}	0.073
$^{176}Hg \rightarrow {}^{172}Pt + \alpha$	6.8990	0^+	0^+	0	2.16×10^{-2}	2.95×10^{-3}	0.137
$^{177}Hg \rightarrow {}^{173}Pt + \alpha$	6.7400	$(7/2^-)^\dagger$	$(5/2^-)$	2	1.39×10^{-1}	1.05×10^{-2}	0.075
$^{178}Hg \rightarrow {}^{174}Pt + \alpha$	6.5770	0^+	0^+	0	3.81×10^{-1}	4.03×10^{-2}	0.106
$^{179}Hg \rightarrow {}^{175}Pt + \alpha$	6.3500	$(7/2^-)[5/2^{-*}]$	$7/2^-$	0[2*]	1.91×10^{0}	2.94×10^{-1}	0.154
$^{180}Hg \rightarrow {}^{176}Pt + \alpha$	6.2585	0^+	0^+	0	5.39×10^{0}	6.62×10^{-1}	0.123

TABLE I. (*Continued.*)

Reaction	$Q_\alpha^{\rm expt}$ (MeV)	J_i^π	J_f^π	$\ell_{\rm min}$	$T_{1/2}^{\rm expt}$ (s)	$T_{1/2}^{\rm calc}$ (s)	S_α
^{181}Hg $\rightarrow$ ^{177}Pt + α	6.2840	$1/2^-$	$5/2^-$	2	1.33×10^{1}	5.04×10^{-1}	0.038
^{182}Hg $\rightarrow$ ^{178}Pt + α	5.9960	0^+	0^+	0	7.22×10^{1}	7.83×10^{0}	0.108
^{183}Hg $\rightarrow$ ^{179}Pt + α	6.0380	$1/2^-$	$1/2^-$	0	8.55×10^{1}	4.98×10^{0}	0.058
^{184}Hg $\rightarrow$ ^{180}Pt + α	5.6620	0^+	0^+	0	2.78×10^{3}	2.41×10^{2}	0.087
^{185}Hg $\rightarrow$ ^{181}Pt + α	5.7740	$1/2^-$	$1/2^-$	0	8.47×10^{2}	6.96×10^{1}	0.082
^{186}Hg $\rightarrow$ ^{182}Pt + α	5.2040	0^+	0^+	0	4.14×10^{5}	4.74×10^{4}	0.115
^{187}Hg $\rightarrow$ ^{183}Pt + α	5.2300	$3/2^{(-)\dagger}$	$1/2^-$	2	3.89×10^{7}	6.33×10^{4}	0.002
^{188}Hg $\rightarrow$ ^{184}Pt + α	4.7030	0^+	0^+	0	5.27×10^{8}	3.81×10^{7}	0.072
^{178}Pb $\rightarrow$ ^{174}Hg + α	7.7900	0^+	0^+	0	1.2×10^{-4}	2.68×10^{-5}	0.223
^{179}Pb $\rightarrow$ ^{175}Hg + α	7.5980	$(9/2^-)$	$(7/2^-)$	2	3.50×10^{-3}	1.81×10^{-4}	0.052
^{180}Pb $\rightarrow$ ^{176}Hg + α	7.4190	0^+	0^+	0	4.20×10^{-3}	3.45×10^{-4}	0.082
^{181}Pb $\rightarrow$ ^{177}Hg + α	7.2400	$(9/2^-)$	$(7/2^-)$	2	3.60×10^{-2}	2.36×10^{-3}	0.066
^{182}Pb $\rightarrow$ ^{178}Hg + α	7.0660	0^+	0^+	0	5.61×10^{-2}	4.78×10^{-3}	0.085
^{183}Pb $\rightarrow$ ^{179}Hg + α	6.9280	$(3/2^-)^\dagger$	$(7/2^-)$	2	8.11×10^{-1}	2.62×10^{-2}	0.032
^{184}Pb $\rightarrow$ ^{180}Hg + α	6.7740	0^+	0^+	0	6.13×10^{-1}	4.91×10^{-2}	0.080
^{185}Pb $\rightarrow$ ^{181}Hg + α	6.6950	$3/2^-$	$1/2^-$	2	1.85×10^{1}	1.74×10^{-1}	0.009
^{186}Pb $\rightarrow$ ^{182}Hg + α	6.4700	0^+	0^+	0	1.21×10^{1}	6.66×10^{-1}	0.055
^{187}Pb $\rightarrow$ ^{183}Hg + α	6.3930	$(13/2^+)^\dagger$	$1/2^-$	7	1.53×10^{2}	4.28×10^{2}	2.804
^{188}Pb $\rightarrow$ ^{184}Hg + α	6.1090	0^+	0^+	0	2.70×10^{2}	1.95×10^{1}	0.072
^{189}Pb $\rightarrow$ ^{185}Hg + α	5.8700	$(3/2^-)$	$1/2^-$	2	3.90×10^{3}	4.16×10^{2}	0.107
^{190}Pb $\rightarrow$ ^{186}Hg + α	5.6970	0^+	0^+	0	1.78×10^{4}	1.40×10^{3}	0.079
^{191}Pb $\rightarrow$ ^{187}Hg + α	5.4600	$(3/2^-)^\dagger$	$3/2^{(-)}$	0	7.98×10^{5}	2.07×10^{4}	0.026
^{192}Pb $\rightarrow$ ^{188}Hg + α	5.2210	0^+	0^+	0	3.56×10^{6}	3.80×10^{5}	0.107
^{185}Bi $\rightarrow$ ^{181}Tl + α	8.1400	$1/2^+$	$(1/2^+)$	0	5.80×10^{-4}	5.20×10^{-6}	0.009
^{187}Bi $\rightarrow$ ^{183}Tl + α	7.7790	$(9/2^-)^\dagger$	$(1/2^+)$	5	3.70×10^{-2}	1.09×10^{-3}	0.029
^{189}Bi $\rightarrow$ ^{185}Tl + α	7.2680	$(9/2^-)^\dagger$	$(1/2^+)$	5	1.50×10^{1}	4.37×10^{-2}	0.003
^{191}Bi $\rightarrow$ ^{187}Tl + α	6.7780	$(9/2^-)^\dagger$	$(1/2^+)$	5	2.43×10^{1}	2.27×10^{0}	0.093
^{193}Bi $\rightarrow$ ^{189}Tl + α	6.3040	$(9/2^-)^\dagger$	$(1/2^+)$	5	7.07×10^{4}	1.63×10^{2}	0.002
^{195}Bi $\rightarrow$ ^{191}Tl + α	5.8320	$(9/2^-)^\dagger$	$(1/2^+)$	5	6.78×10^{6}	1.96×10^{4}	0.003
^{197}Bi $\rightarrow$ ^{193}Tl + α	5.3650	$(9/2^-)^\dagger$	$(1/2^+)$	5	5.60×10^{8}	4.25×10^{6}	0.008

for the α particle as [29]

$$\rho_\alpha(\vec{r},\vec{r}+\vec{s}) \simeq \rho_\alpha\left(\left|\vec{r}+\frac{\vec{s}}{2}\right|\right)\exp\left(-\frac{s^2}{4\,b_\alpha^2}\right), \qquad (11)$$

where b_α is equal to 1.1932 fm.

To accelerate the convergence of the density matrix expansion, Campi and Bouyssy [31] have suggested to choose, for a spherically symmetric ground-state density, the local Fermi momentum, $k_{\rm eff}(r)$, in the following form:

$$k_{\rm eff}(r) = \left\{\frac{5}{3\rho(r)}\left[\tau(r) - \frac{1}{4}\nabla^2\rho(r)\right]\right\}^{1/2}. \qquad (12)$$

Using the extended Thomas-Fermi approximation, the kinetic energy density is then given by

$$\tau(r) = \frac{3}{5}\left(\frac{3\pi^2}{2}\right)^{2/3}\rho(r)^{5/3} + \frac{1}{3}\nabla^2\rho(r) + \frac{1}{36}\frac{|\,\vec{\nabla}\rho(r)\,|^2}{\rho(r)}. \qquad (13)$$

The first term in this expression stands for Thomas-Fermi approximation while the other two terms represent the surface correction.

A realistic NN interaction is used in our calculations, whose parameters reproduce consistently the equilibrium density and the binding energy of normal nuclear matter as well as the density and energy dependence of the nucleon-nucleus optical potential. The density-dependent M3Y-Paris effective NN force considered in the present work, CDM3Y1, has the factorized form [32]

$$\upsilon_D(\rho,E,s) = \left[11061.625\,\frac{e^{-4s}}{4\,s} - 2537.5\,\frac{e^{-2.5s}}{2.5\,s}\right]F(\rho)\,g(E), \qquad (14)$$

$$\upsilon_{Ex}(\rho,E,s) = \left[-1524.25\,\frac{e^{-4s}}{4\,s} - 518.75\,\frac{e^{-2.5s}}{2.5\,s} - 7.8474\,\frac{e^{-0.7072s}}{0.7072\,s}\right]F(\rho)\,g(E), \qquad (15)$$

with the density and energy dependence, respectively,

$$F(\rho) = c[1 + \alpha\exp(-\beta\rho) - \gamma\rho], \qquad (16)$$

$$g(E) = (1 - 0.003\,E_{Ap}), \qquad (17)$$

The parameters c, α, β, and γ are adjusted to reproduce normal nuclear matter saturation properties for a given equation of state for cold nuclear matter. For CDM3Y1, $c = 0.3429$, $\alpha = 3.0232$, $\beta = 3.5512\,{\rm fm}^3$, and $\gamma = 0.5\,{\rm fm}^3$, which generate a nuclear matter equation of state with the incompressibility

value $K = 188$ MeV. E_{Ap} is the incident energy per projectile nucleon in the laboratory system.

Assuming the local approximation, Eq. (9), and using the energy and density-dependent exchange interaction $\upsilon_{Ex}(\rho,E,s)$, one easily obtains the self-consistent and local exchange potential V_{Ex} as [29]

$$V_{\rm Ex}(E,R) = 4\pi \int_0^\infty ds\, s^2\, \upsilon_{\rm Ex}(\rho,E,s)\, j_0(k(E,R)s/M) \times \int \mathrm{d}\vec{y}\, \rho_d(|\vec{y}-\vec{R}|)\, \hat{j}_1(k_{\rm eff}(|\vec{y}-\vec{R}|)s) \times \rho_\alpha(y) \exp\left(-\frac{s^2}{4\,b_\alpha^2}\right). \quad (18)$$

The exchange potential, Eq. (18), can then be evaluated by an iterative procedure which converges very fast.

Finally, the obtained α-daughter interaction potential is employed to compute the barrier penetrability, Eq. (2), and the assault frequency, Eq. (3), which are used in turn to obtain the α decay half-life time. Now, the calculated half-lives, without S_α, and the experimental ones allow for deducing the preformation probability of the α cluster inside the parent nucleus as [22,33]

$$S_\alpha = T_{1/2}^{\rm calc} / T_{1/2}^{\rm expt}. \quad (19)$$

III. RESULTS AND DISCUSSION

The α-particle preformation probability is extracted from the recent experimental α decay half-life [34] and the penetration probability is obtained from the WKB approximation in combination with the Bohr-Sommerfeld quantization condition. The microscopic α-nucleus potential is numerically constructed in the well-established double-folding model derived from a realistic density-dependent effective CDM3Y1-Paris NN interaction [32] with a finite-range exchange force. The main effect of antisymmetrization under exchange of nucleons between the α and the daughter nuclei has been included in the folding model through the finite-range exchange part of the NN interaction.

We studied the variation of S_α with the neutron number of the parent nucleus for α emitters with $74 \leqslant Z \leqslant 83$. A difficulty in the present work is that the spin and parity assignments of the parent and daughter nuclei, J^π, are probably not accurate. The value of J^π is used to determine the α particle angular momentum which affects the value of S_α. Thus if the value of J^π is not correct for a particular nucleus, this will be reflected on the value of S_α at this point and the behavior of S_α for this nucleus will be incorrect. Figure 1 shows the variation of S_α for the ^{167}Pt nucleus, as an example, with ℓ value. It shows that S_α increases with ℓ value.

It should be noted that, for nuclei far from shell closure, the understanding of the role played by configuration mixing to induce the clustering of the four nucleons that would eventually constitute the α particle posed a major problem within the shell approach. It was found that, with the participation of high-lying configurations within shell model, the pairing interaction enhances the α decay width and clusters the two neutrons and the two protons on the nuclear surface [35]. Yet,

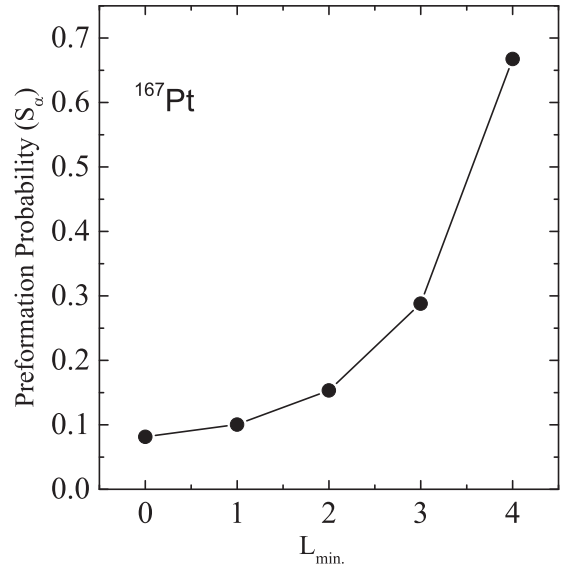

FIG. 1. The variation of S_α for the ^{167}Pt nucleus, as an example, with ℓ value.

the eventual clustering of the α particle is produced when the proton-neutron (p-n) interaction is included.

Figure 2 shows the variation of S_α with neutron number for the Bi and Pb isotopes. The present analysis is based on assuming that the states of the parent nucleus consist of a few valence configurations which determine its spin and parity in the framework of the independent particle model. The level sequences and occupation number of levels are deduced from the spin and parity assignments of the parent and daughter nuclei and, in some cases, they are confirmed by the tabulated values of the spin and parity of the neighboring isotones and/or isotopes of the parent nucleus. The net spin in odd-A nuclei is almost always determined by the unpaired nucleon with

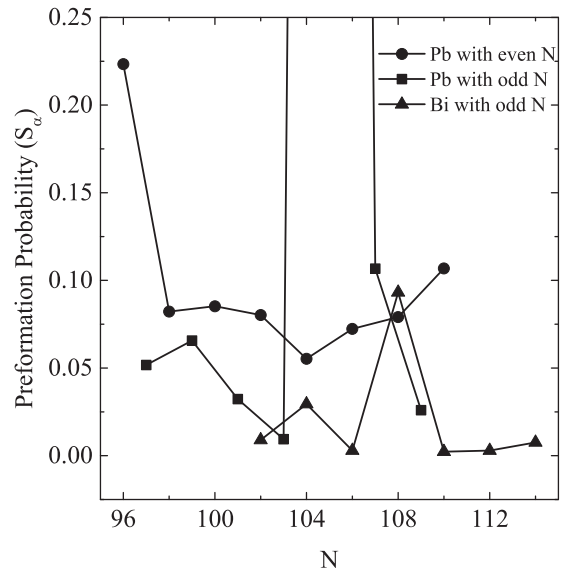

FIG. 2. Extracted α-preformation probability, S_α, for different isotopes of Pb and Bi nuclei with the parent neutron number N.

remaining nucleons pairing to zero spin. For example, the odd-A $^{187-197}$Bi nuclei with neutron numbers in the range $N = 104-114$ have $J^\pi = 9/2^-$. This means that the unpaired proton in these nuclei occupies the level $1h_{9/2}$, and when the α particle is emitted the spin of the daughter nucleus becomes $1/2^+$. Thus the uppermost proton levels of the parent nuclei are $1h_{9/2}$ and $3s_{1/2}$; the first level has odd number of protons which determines J^π of the parent nucleus, while the second level has two protons. So, the ground-state α transition ($9/2^- \rightarrow 1/2^+$) of $^{187-197}$Bi should take the unpaired proton from the $1h_{9/2}$ orbit and one proton from the $3s_{1/2}$ orbit leaving the $3s_{1/2}$ orbit with an unpaired proton. Therefore, the proton pair in the α decay of $^{187-197}$Bi nuclei is assumed to come from $1h_{9/2}$ and $3s_{1/2}$ levels. When the neutron number decreases to 102, the spin of the parent nucleus becomes $1/2^+$ and the proton pair comes from the level $1h_{9/2}$.

Compared to the behavior of S_α for element Po [24], in the neutron number variation range 106 to 114, one can say that the neutron pair in the α emission process from Bi isotopes with neutron numbers $N = 114$, 112, and 110 comes from the level $3p_{3/2}$. For $N = 108$, the proton pair comes from the level $1i_{13/2}$, while for $N = 106$, it comes again from the level $3p_{3/2}$ (the spin of ^{193}Po$_{109}$ is $13/2^+$ and that of ^{191}Po$_{107}$ is $3/2^-$). The neutron levels, in this case, are similar to Po levels in this neutron variation range; the level $3p_{3/2}$ is filled by neutrons more than one time. The p-n interaction is known to be orbit sensitive and, nearly independent of the details of the interaction, is largest for orbits of large spatial overlap. A useful measure for the average strength of proton-neutron interaction, which plays an important role in the behavior of S_α, is given by the average value [36–38] $f_{np} = (\frac{1}{1+\triangle n+\triangle \ell+\triangle j})_{\rm avg}$, where $\triangle n$, $\triangle \ell$, and $\triangle j$ are the differences in quantum numbers n, ℓ, and j, respectively, of the levels occupied by protons and neutrons. The average is taken over the two protons and two neutrons energy levels. The measure f_{np} of the proton-neutron interaction is 0.217 for $N = 114$, 112, 110, and 106, while it is reduced to 0.158 for $N = 108$. The small increase of S_α at $N = 104$ is probably due to the contribution of the $1i_{13/2}$ neutron level again to the emission process. Thus, the behavior of S_α for Bi isotopes confirm the values of spins as shown in Table I.

For Pb isotopes with odd neutron number, a sudden jump in the value of S_α appears at $N = 105$. This sudden jump occurs when the neutron level $1i_{13/2}$ contributes to the α emission, as we found in element Po. Above this level is the $3p_{3/2}$ level which contributes several times to the α emission. The Pb isotopes with neutron numbers $N = 109$, 103, and 101 have $J^\pi = 3/2^-$ (the values of S_α for these neutron numbers are almost the same), and for $N = 105$ the value of J^π of the ^{187}Pb isotope is $13/2^+$. The neutron level $3/2^-$ may contribute again to the α emission at $N = 107$, where the value of S_α is increased to about 0.1, but this was found in the Po nucleus [24]. It should be noted that f_{np} for the neutron-proton levels $3p_{3/2}-3s_{1/2}$ has a value 0.333, while for the levels $1i_{13/2}-3s_{1/2}$ it is reduced to 0.067. For $N = 97$ and 99, the odd neutron changed level probably to $5/2^-$ or $9/2^-$. S_α for these two points has almost the same value, which means an equal value of J^π. The behavior of S_α for even-N Pb isotopes differs considerably from the same quantity for odd-N Pb isotopes. This indicates that the neutron levels of even-N Pb isotopes differ from the levels of odd-N Pb isotopes. In the neutron number range $N = 106-110$, the behavior of S_α for Pb isotopes is almost the same as the behavior for Po isotopes [24], indicating that the neutron levels in the two elements, Pb and Po, are almost the same in this neutron number range. Thus the variation of S_α for Pb isotopes with the neutron number predicts that the odd-N -isotopes ^{191}Pb, ^{189}Pb, ^{185}Pb, and ^{183}Pb have $J^\pi = 3/2^-$ and the ^{187}Pb isotope has $J^\pi = 13/2^+$. This agrees with the values of J^π in Table I.

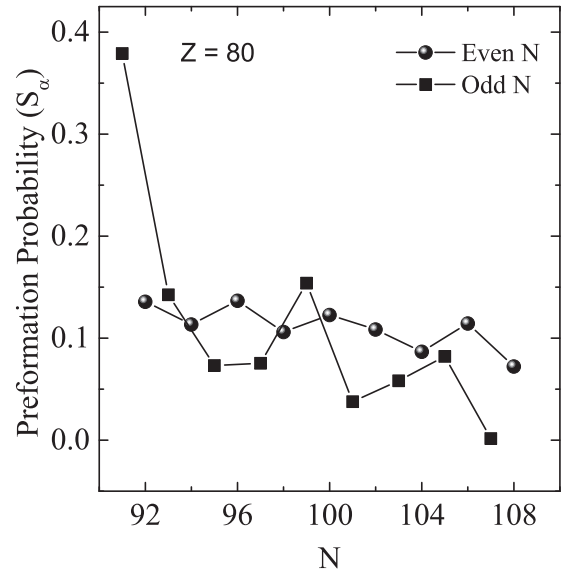

FIG. 3. The same as Fig. 2 but for Hg isotopes.

Figure 3 shows our calculations for the Hg isotopes. For $N = 107$, the tabulated value of J^π for the ^{187}Hg isotope is $3/2^-$. This value is confirmed for the three elements Rn, Po, and Pb with the same neutron number $N = 107$, where their spin-parity assignments are $3/2^-$. The proton pair is emitted from the level $3s_{1/2}$ because the spins of Tl isotopes with neutron number in the range $N = 100-108$ are $1/2^+$. Since the daughter nucleus has spin $1/2^-$, it is reasonable to emit one neutron from the level $3p_{1/2}$ and the other neutron from the level $3p_{3/2}$. For these levels, $f_{np} = 0.417$. For $N = 101$, 103, and 105, the spin of $^{181-185}$Hg isotopes is confirmed and its value is $1/2^-$, which means that the neutron pair in the α emission comes from the two levels $3p_{1/2}$ and $2f_{5/2}$. The f_{np} for this emission has a value 0.321, which explains the small increase of S_α at $N = 105$. The $3p_{1/2}$ level is occupied again by neutrons at $N = 103$ and 101; it contributes three times to the emission process, producing holes below. The contribution of the $3p_{1/2}$ level produces, several times, a slow decrease of S_α with lowering N value. It should be noted that the $3p_{1/2}$ neutron level contributed to the α emission, for the nuclei with $Z \geqslant 84$ [24], only one time below the neutron magic number $N = 126$.

For ^{179}Hg isotope with $N = 99$, the value of S_α increases at this point, indicating that the n-p interaction becomes smaller. Thus we confirm the value $J^\pi = 5/2^-$ for ^{179}Hg isotope, because it lowers f_{np} to a value of 0.143, which is less than half its value for $N = 101$. For $N = 97$ and 95, $J^\pi = 7/2^-$;

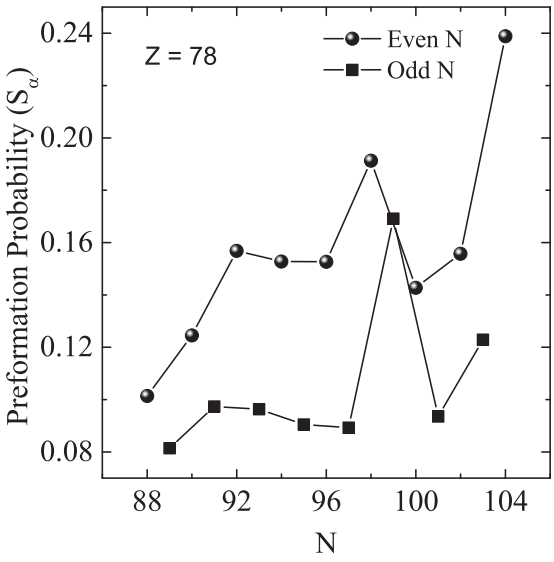

FIG. 4. The same as Fig. 2 but for Pt isotopes.

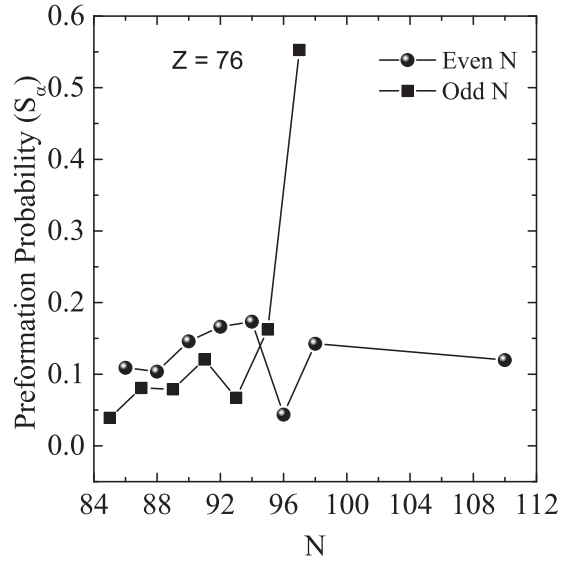

FIG. 5. The same as Fig. 2 but for Os isotopes.

this value decreases f_{np} to 0.125. The decrease in the value of S_α at $N = 95$ and 97 is due to the change in the emission level and the presence of holes in the level $2f_{5/2}$. Moreover, the proton level may be changed at the above mentioned N values [the spin of ^{177,179}Tl for N values 96 and 98 is $1/2^+$; the spin of $^{175}Au_{96}$ is $1/2^+$; the spin of $^{177}Au_{98}$ is ($1/2^+$, $3/2^+$), and the spin $^{173}Au_{94}$ is $1/2^+$]. The values of S_α at $N = 95$ and 97 are almost the same, which means that the neutron levels at $N = 95$ and 97 are the same. For $N = 93$, S_α has almost the same value as $N = 99$, indicating that the spin is $5/2^-$. The Hg isotope with $N = 91$ has a value of S_α about 0.38; this large value was found in the isotope of Po [24], ^{191}Po, emitting its two neutrons from the level $3p_{3/2}$ (S_α in this case is 0.56). Therefore, the neutron level may be $3/2^-$ at $N = 91$ as tabulated. Thus the behavior of S_α for odd neutron number variation can confirm the recent tabulated spins except for ^{173}Hg and ^{179}Hg isotopes. These isotopes have spins $J^\pi = 5/2^-$ instead of $7/2^-$. These spin values are consistent with the confirmed spins of Pt isotopes which produce the same behavior of S_α as the corresponding Hg isotopes. The variation of S_α for the even neutron number Hg isotopes is too slow compared to the odd neutron number Hg isotopes, indicating that differences exist in structure between even and odd isotopes.

Figure 4 is the same as Fig. 3 except it is for the Pt isotopes. The confirmed spins of the Pt isotopes indicate that the neutron levels $3p_{1/2}$, $2f_{7/2}$, and $2f_{5/2}$ contribute to the emission process. The variation of S_α for the odd neutron number Pt isotopes in the neutron range $N = 95-103$ is almost similar to the corresponding variation of S_α for Hg isotopes. Moreover, the values of the corresponding points in the two figures are almost equal. This shows almost similar proton and neutron level sequences for Pt and Hg isotopes in the neutron variation range $N = 95-103$. For element Pt, the spins of the isotopes with $N = 103$, 101, 99, and 97 are precisely determined and their values are, respectively, $1/2^-$, $1/2^-$, $5/2^-$, and $7/2^-$.

For Pt isotopes with $N < 97$, S_α becomes almost constant, which means the emission of proton and neutron pairs comes from the same levels. Thus for the isotopes ^{173}Pt, ^{171}Pt, and ^{169}Pt the spins are equal and have the same value as ^{175}Pt, which has the confirmed value $J^\pi = 7/2^-$. Since the level $2f_{7/2}$ can be filled by eight neutrons, the ^{167}Pt isotope with $N = 89$ may have a value $J^\pi = 7/2^-$, and in this case the level $2f_{7/2}$ has two neutrons from the lower levels. It should be noted that the neutron level $3p_{1/2}$, which contributed to α emission just below the magic number $N = 126$ for heavy elements with $Z \geqslant 84$, appeared in the present study several times at smaller values of N. S_α for this level decreases slowly with decreasing number of neutrons. The behavior of even neutron number Pt isotopes is almost the same as odd neutron number isotopes but shifted one neutron to the left. This means that both even and odd neutron number Pt isotopes have the same proton and neutron level sequences (the structure of odd neutron number Pt isotopes is not affected by the addition of one neutron).

Figure 5 shows the results of element Os with $Z = 76$. The two f levels, $2f_{5/2}$ and $2f_{7/2}$, contribute to the emission process in the odd neutron number variation range 97–85. These levels appeared in $Z = 78$ element in the range $N = 89-99$. The tabulated values of J^π for $N = 97$, 95, and 93 is $5/2^-$ and S_α decreases with decreasing value of N. Comparing to Fig. 4, the value of S_α at $N = 95$ for element Os is almost equal to the corresponding value of S_α for element Pt at $N = 99$ in Fig. 4. This shows that the spin of Os with $N = 95$ is $5/2^-$. Thus the level $2f_{5/2}$ contributed twice in emission process, one at $N = 97$ with a too large value of S_α and the other at $N = 95$, where S_α has almost the same value as ^{177}Pt. The large drop in the value of S_α at $N = 95$ is probably due to change in the proton levels [J^π for ^{175}Ir, ^{173}Ir, ^{171}Ir is $5/2^-$, ($5/2^+$,$3/2^+$), $1/2^+$, and for ^{171}Re, ^{169}Re it is $5/2^-$, $9/2^-$, respectively). For $N = 93$, 91, 89, 87, and 85, the values of S_α and its behavior with decreasing N value are almost the same as the emission from the $2f_{7/2}$ level for Pt isotopes presented in Fig. 4. Thus,

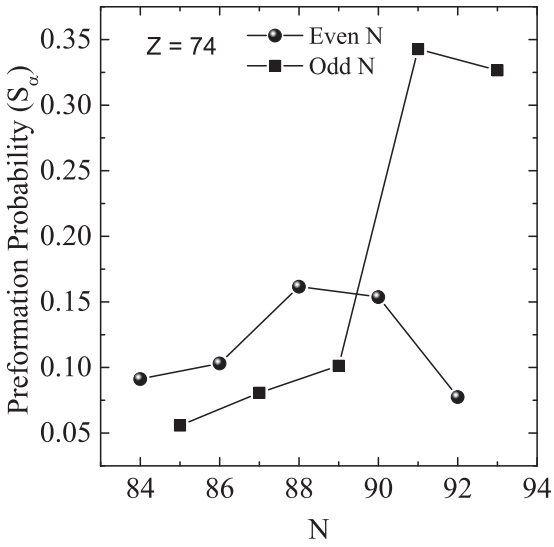

FIG. 6. The same as Fig. 2 but for W isotopes.

we can assign the value $J^\pi = 7/2^-$ for the isotopes of element Os with odd neutron numbers $N = 85-93$. Since the level $2d_{7/2}$ is filled with eight neutrons, we assume that it has two extra neutrons from a lower level. The proton level for this emission is $3s_{1/2}$, and S_α varies slowly with N. The values of S_α in this case are almost the same as Pt isotopes. The variation of S_α for even neutron number Os isotopes for $N = 86-94$ is almost the same as for odd neutron number Os isotopes in the range $N = 85-93$.

For W isotopes, shown in Fig. 6, the three points at $N = 85$, 87, and 89 have almost the same values of S_α as the corresponding points in Os isotopes. This means that the value of J^π of ^{159}W, ^{161}W, and ^{163}W is $7/2^-$. For $N = 91$ and 93, S_α is almost the same and its value is about 0.35. Comparing to Hg isotopes with $N = 91$ (the value of S_α is about 0.35), we can deduce that J^π for the two isotopes, ^{165}W and ^{167}W, is the same as J^π for ^{171}Hg which may be $3/2^-$. The variation of S_α for even neutron number W isotopes with $N = 84$, 86, and 88 is almost the same as for odd neutron number W isotopes with $N = 85$, 87, and 89, indicating similar levels for these isotopes.

IV. SUMMARY AND CONCLUSION

We investigated the dependence of the preformation probability of an α cluster on the neutron number of the parent nucleus for α emitters with $74 \leqslant Z \leqslant 83$. The α-particle preformation probability is extracted from the recently observed experimental α decay half-life, and the penetration probability is obtained from the WKB approximation in combination with the Bohr-Sommerfeld quantization condition.

In the present study, we compared the values and behavior of S_α for different isotopes of an element with those of another element. Based on the equality in the values of S_α for two different elements and the tabulated values of spins, we correlate the energy levels of the two elements. Also similarity in the behavior of S_α with the neutron number variation, for two adjacent elements, means similar energy levels for the elements. In some cases, we used a simple measure of n-p interaction to interpret the increase or decrease in the value of S_α. We found that the variation of S_α for odd neutron number isotopes of the element Pt is exactly the same as for even neutron number isotopes. This indicates that the addition of one neutron to an odd neutron isotope of element Pt does not change its valence levels. As in our previous work [24], we found that the emission from the neutron level $1i_{13/2}$ is accompanied by a large increase in the value of S_α, and the level $3p_{1/2}$ contributed several times tothe emission process in the atomic number region $74 \leqslant Z \leqslant 83$. The $3p_{1/2}$ neutron energy level contributed to α emission for nuclei with $Z \geqslant 84$ only one time below the neutron magic number $N = 126$.

[1] Y. Qian, Z. Ren, and D. Ni, Phys. Rev. C **89**, 024318 (2014).
[2] D. Bucurescu and N. V. Zamfir, Phys. Rev. C **87**, 054324 (2013).
[3] D. Ni and Z. Ren, Phys. Rev. C **87**, 027602 (2013).
[4] D. Ni, Z. Ren, T. Dong, and Y. Qian, Phys. Rev. C **87**, 024310 (2013).
[5] M. Ismail and A. Adel, Phys. Rev. C **88**, 054604 (2013)
[6] S. Hofmann and G. Munzenberg, Rev. Mod. Phys. **72**, 733 (2000).
[7] P. E. Hodgeson and E. Betak, Phys. Rep. **374**, 1 (2003).
[8] M. Ismail, A. Y. Ellithi, M. M. Botros, and A. Adel, Phys. Rev. C **81**, 024602 (2010).
[9] W. M. Seif, Phys. Rev. C **74**, 034302 (2006).
[10] Yu. Ts. Oganessian *et al.*, Phys. Rev. C **87**, 054621 (2013).
[11] Yu. Ts. Oganessian *et al.*, Phys. Rev. Lett. **104**, 142502 (2010).
[12] Yu. Ts. Oganessian *et al.*, Phys. Rev. C **74**, 044602 (2006).
[13] G. Gamow, Z. Phys. **51**, 204 (1928).
[14] G. Royer, J. Phys. G: Nucl. Part. Phys. **26**, 1149 (2000).
[15] C. Xu and Z. Ren, Nucl. Phys. A **753**, 174 (2005).
[16] D. S. Delion, S. Peltonen, and J. Suhonen, Phys. Rev. C **73**, 014315 (2006).
[17] S. Peltonen, D. S. Delion, and J. Suhonen, Phys. Rev. C **75**, 054301 (2007).
[18] K. P. Santhosh, J. G. Joseph, and S. Sahadevan, Phys. Rev. C **82**, 064605 (2010).
[19] K. P. Santhosh and B. Priyanka, Phys. Rev. C **87**, 064611 (2013).
[20] K. P. Santhosh and B. Priyanka, Phys. Rev. C **89**, 064604 (2014).
[21] H. F. Zhang and G. Royer, Phys. Rev. C **77**, 054318 (2008).
[22] W. M. Seif, M. Shalaby, and M. F. Alrakshy, Phys. Rev. C **84**, 064608 (2011).
[23] W. M. Seif, J. Phys. G: Nucl. Part. Phys. **40**, 105102 (2013).
[24] M. Ismail and A. Adel, Phys. Rev. C **86**, 014616 (2012).
[25] M. Ismail and A. Adel, Nucl. Phys. A **912**, 18 (2013).
[26] N. G. Kelkar and H. M. Castaneda, Phys. Rev. C **76**, 064605 (2007).
[27] G. R. Satchler and W. G. Love, Phys. Rep. **55**, 183 (1979).
[28] M. Ismail and A. Adel, Phys. Rev. C **84**, 034610 (2011).
[29] D. T. Khoa, Phys. Rev. C **63**, 034007 (2001).

[30] B. Sinha, Phys. Rep. **20**, 1 (1975).
[31] X. Campi and A. Bouyssy, Phys. Lett. B **73**, 263 (1978).
[32] Dao T. Khoa, G. R. Satchler, and W. von Oertzen, Phys. Rev. C **56**, 954 (1997).
[33] M. Bhattacharya, S. Roy, and G. Gangopadhyaya, Phys. Lett. B **665**, 182 (2008).
[34] NuDat2.6, Nuclear Structure and Decay Data, available from http://www.nndc.bnl.gov/nudat2/
[35] I. Tonozuka and A. Arima, Nucl. Phys. A **323**, 45 (1979).
[36] R. F. Casten, Phys. Lett. B **152**, 145 (1985).
[37] R. F. Casten, Phys. Rev. Lett. **54**, 1991 (1985).
[38] R. F. Casten, Nucl. Phys. A **443**, 1 (1985).